Supplement of

Understanding new particle formation based on continuous nanoparticle ranking in boreal forest and urban megacity

Tinghan Zhang[1,2], Wei Du[3], Xinran Zhang[2], Janne Lampilahti[2], Chengfeng Liu[2], Zehao Zou[2], Men Xia[5], Qi Yuan[1], Qiaozhi Zha[5], Jing Cai[7], Yiyang Wang[6], Tom Kokkonen[2], Katrianne Lehtipalo[2,4], Tuukka Petäjä[2], Veli-Matti Kerminen[2], Chao Yan[5], Jingkun Jiang[6], Yongchun Liu[1] and Markku Kulmala[1,2,5]

[1]Aerosol and Haze Laboratory, Beijing Advanced Innovation Center for Soft Matter Science and Engineering, Beijing University of Chemical Technology, Beijing, China

[2]Institute for Atmospheric and Earth System Research/Physics, Faculty of Science, University of Helsinki, Helsinki, Finland

[3]State Key Laboratory of Atmospheric Environment and Extreme Meteorology, Institute of Atmospheric Physics, Chinese Academy of Sciences, Beijing, 100029, China

[4]Atmospheric Composition Research, Finnish Meteorological Institute, Helsinki, Finland

[5]Nanjing-Helsinki Institute in Atmospheric and Earth System Sciences, Nanjing University, Suzhou, China

[6]School of Environment, State Key Joint Laboratory of Environment Simulation and Pollution Control, Tsinghua University, Beijing, China

[7]State Key Laboratory of Climate System Prediction and Risk Management, Nanjing University of Information Science and Technology, Nanjing, 210044, China

Correspondence to: duwei@mail.iap.ac.cn, jiangjk@tsinghua.edu.cn

Contents of this file

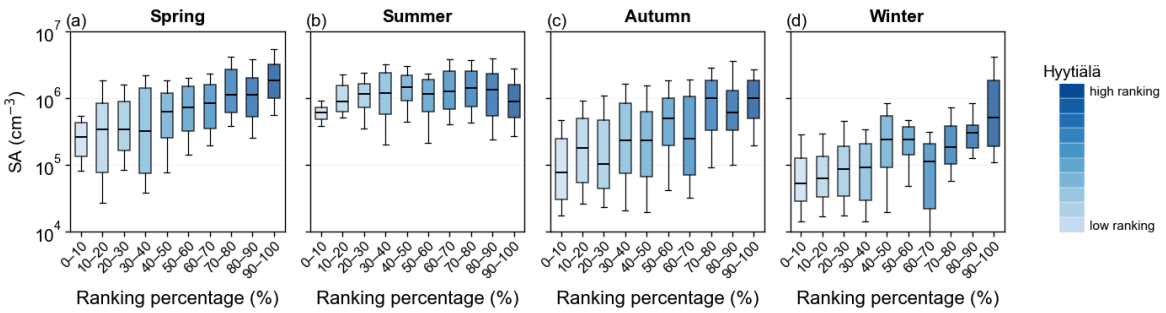

Figure S1. Seasonal evolution of sulfuric acid at Hyytiälä (a-d) as a function of percentile ranking. Each subplot represents one season. The SA values were calculated from data between 09:00 and 17:00 local time. The boxplots show the median (central line), 25th and 75th percentiles (box edges), and the 10th and 90th percentiles (whiskers).

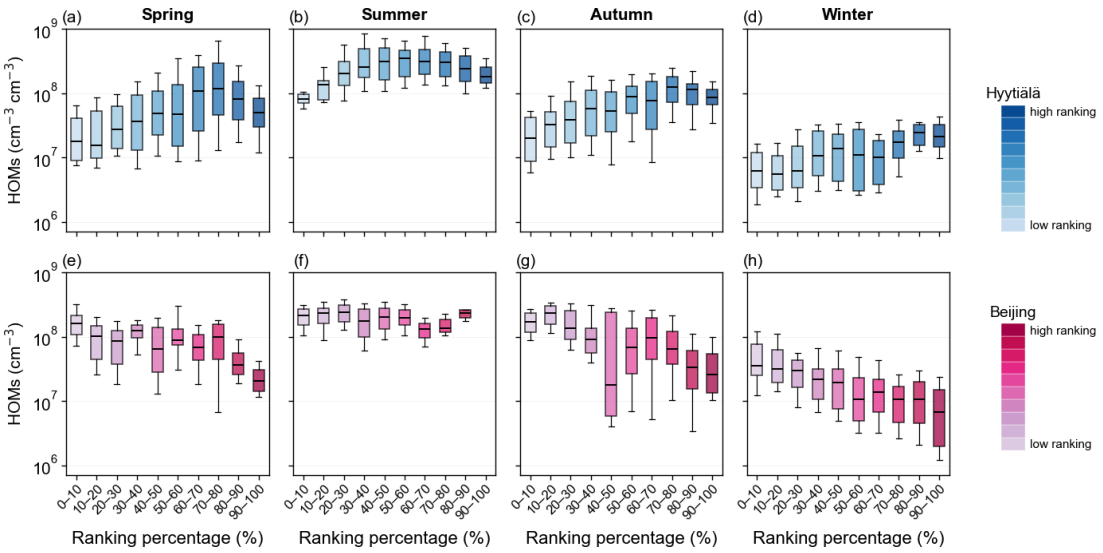

Figure S2. Seasonal evolution of highly oxygenated organic molecules (HOMs) at Hyytiälä (a-d) and Beijing (e-h) as a function of percentile ranking. Each subplot represents one season. The HOMs values were calculated using data between 09:00 and 17:00 local time. The boxplots show the median (central line), 25th and 75th percentiles (box edges), and the 10th and 90th percentiles (whiskers).

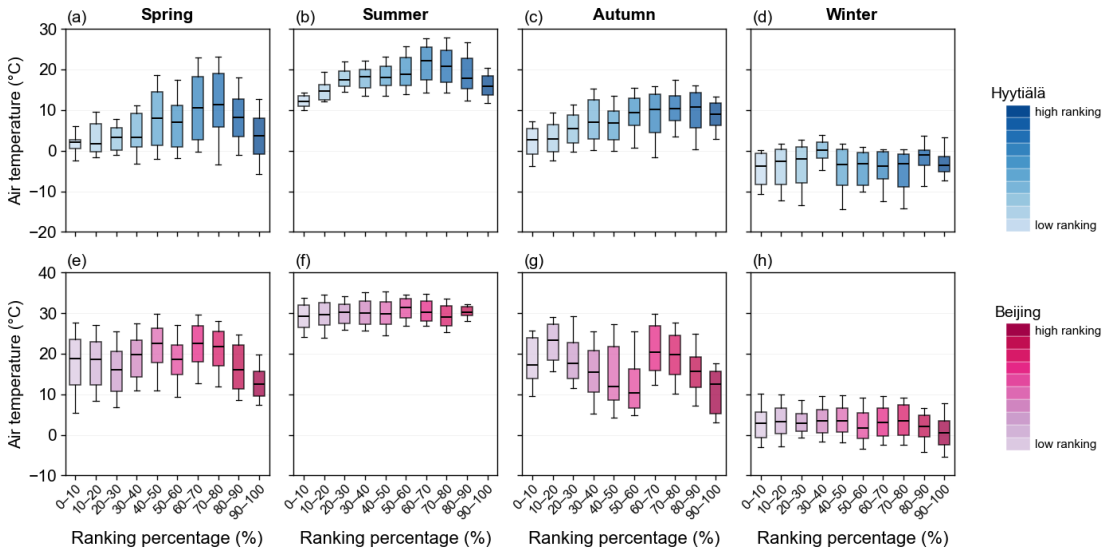

Figure S3. Seasonal evolution of air temperature at Hyytiälä (a-d) and Beijing (e-h) as a function of percentile ranking. Each subplot represents one season. The temperature values were calculated using data between 09:00 and 17:00 local time. The boxplots show the median (central line), 25th and 75th percentiles (box edges), and the 10th and 90th percentiles (whiskers).

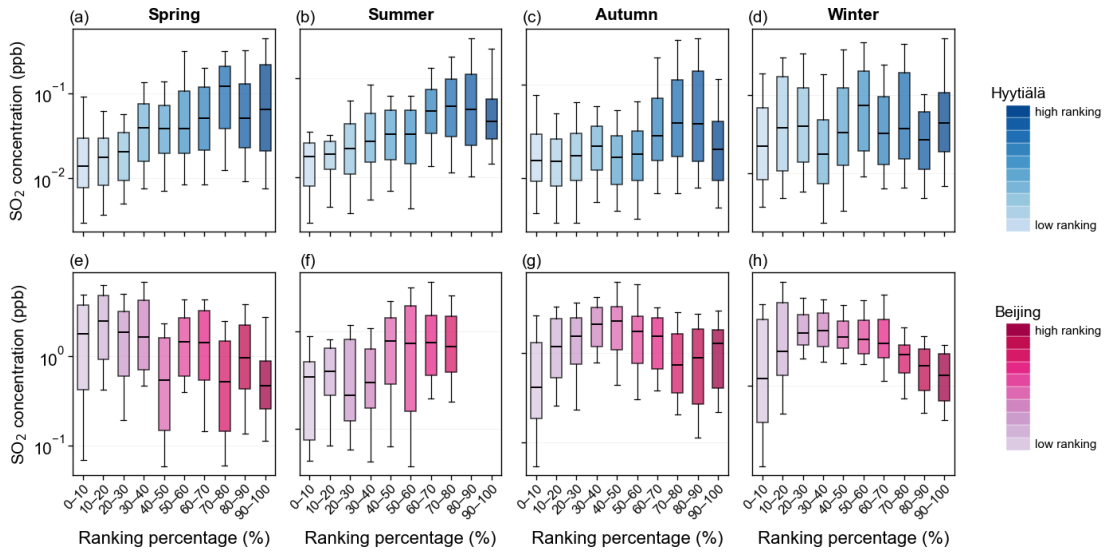

Figure S4. Seasonal evolution of SO_2 at Hyytiälä (a-d) and Beijing (e-h) as a function of percentile ranking. Each subplot represents one season. The SO_2 values were calculated from data between 09:00 and 17:00 local time. The boxplots show the median (central line), 25th and 75th percentiles (box edges), and the 10th and 90th percentiles (whiskers).

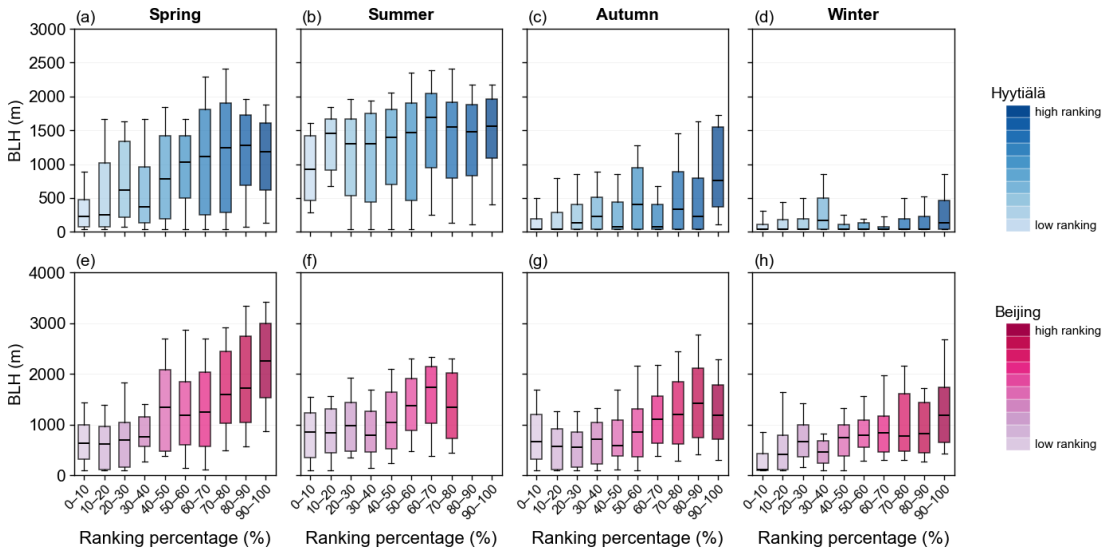

Figure S5. Seasonal evolution of boundary layer height (BLH) as a function of percentile ranking at Hyytiälä (a-d) and Beijing (e-h). Each subplot represents one season. The BLH values were calculated from data between 09:00 and 17:00 local time. The boxplots show the median (central line), 25th and 75th percentiles (box edges), and the 10th and 90th percentiles (whiskers). The boxplot for the 80–90% ranking interval in summer at Beijing was omitted because of the limited number of available data points.

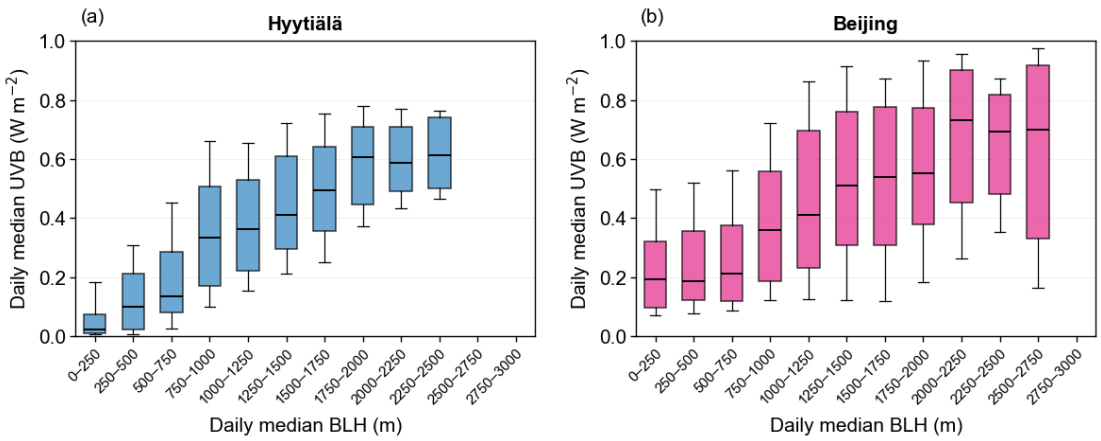

Figure S6. Relationship between daytime UVB and boundary layer height (BLH) at Hyytiälä (a) and Beijing (b). Daily median UVB and BLH values were calculated from data between 09:00 and 17:00 local time. The boxplots show the median UVB values within each daily median BLH interval, with the central line indicating the median, the box edges representing the 25th and 75th percentiles, and the whiskers indicating the 10th and 90th percentiles.

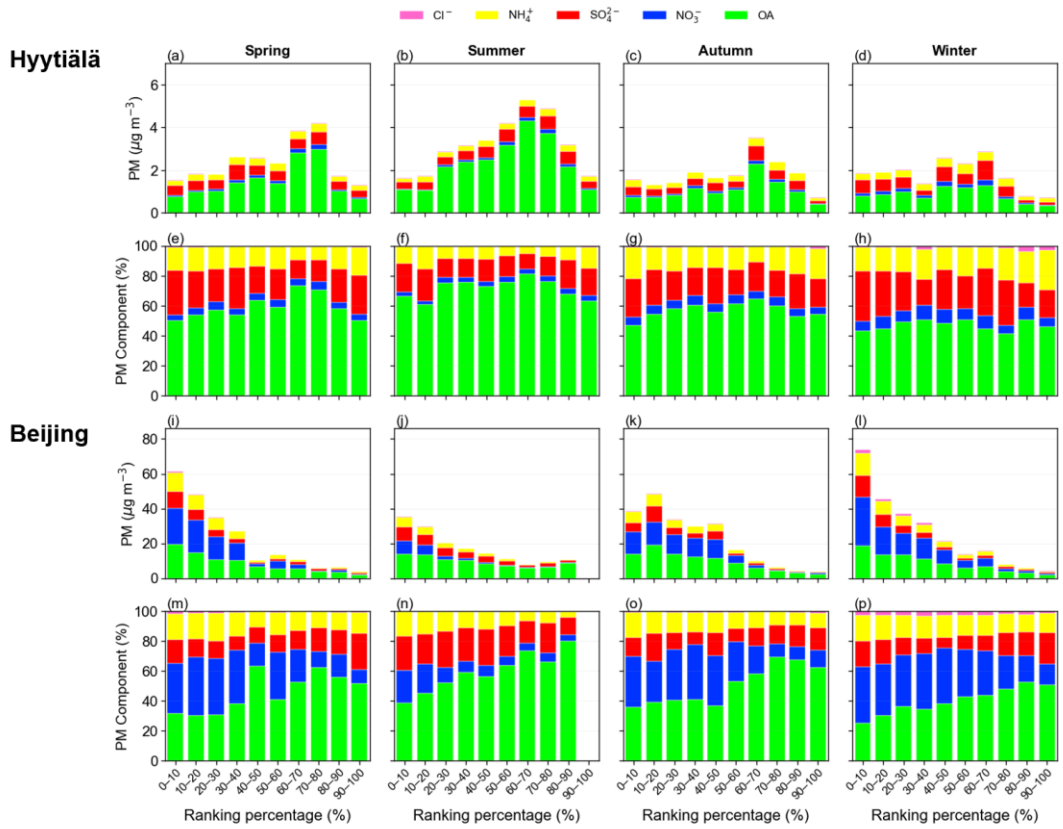

Figure S7. Seasonal variation of PM mass concentrations and chemical composition as a function of percentile ranking at Hyytiälä (a–h) and Beijing (i–p). All values were calculated from data between 09:00 and 17:00 local time. Panels (a–d) and (i–l) show the median PM mass concentrations, while panels (e–h) and (m–p) show the relative contributions of the major PM components, including organic aerosol (OA), nitrate (NO_3^-), sulfate (SO_4^{2-}), ammonium (NH_4^+), and chloride (Cl^-). Each column represents a different season, and the bars correspond to 10 % percentile ranking intervals.

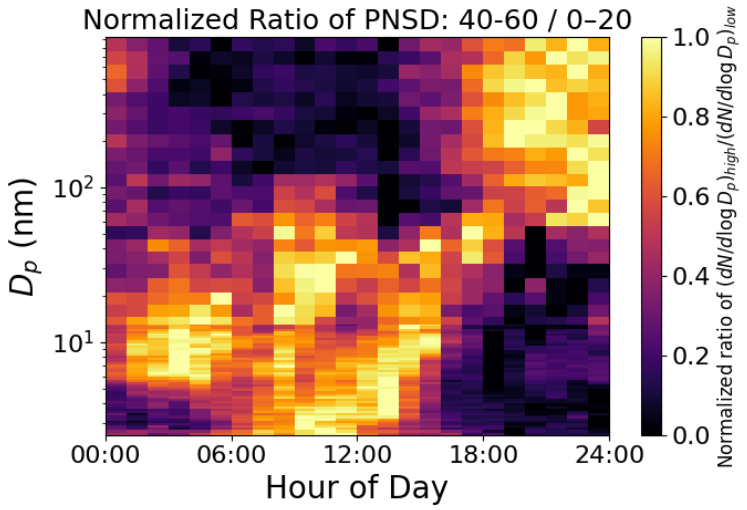

Figure S8. Diurnal variation in the normalized ratio of the median particle number size distributions (PNSDs) between the 40–60 % and 0–20 % ranking intervals in Beijing. The ratio was calculated as $\left(\mathrm{d}N/\mathrm{d}\log D_\mathrm{p}\right)_{40\text{–}60\,\%}/\left(\mathrm{d}N/\mathrm{d}\log D_\mathrm{p}\right)_{0\text{–}20\,\%}$ for each particle size bin and hour of the day and subsequently normalized to the range 0–1.

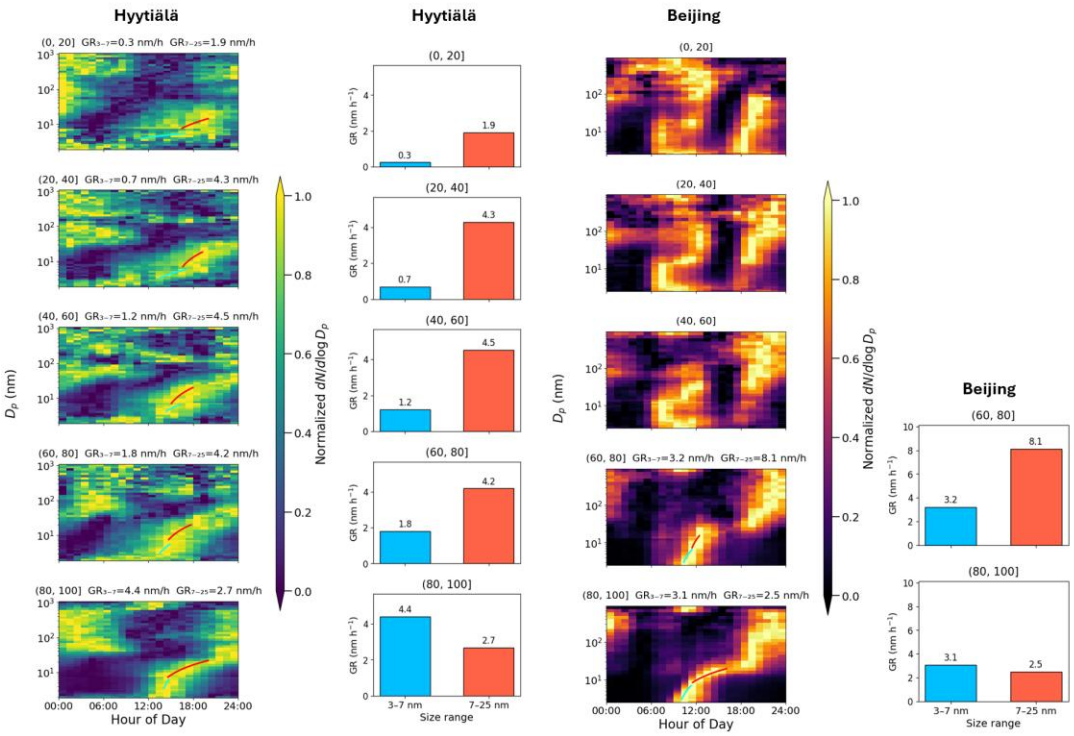

Figure S9. Estimation of growth rates (GR) for 3–7 nm and 7–25 nm particles using the maximum concentration method at Hyytiälä (left) and Beijing (right) for different percentile ranking intervals. The surface plots show the normalized particle number size distributions with fitted growth trajectories. The corresponding GR values derived from the fitting are summarized in the adjacent bar charts for the 3–7 nm (blue bars) and 7–25 nm (red bars) size ranges.

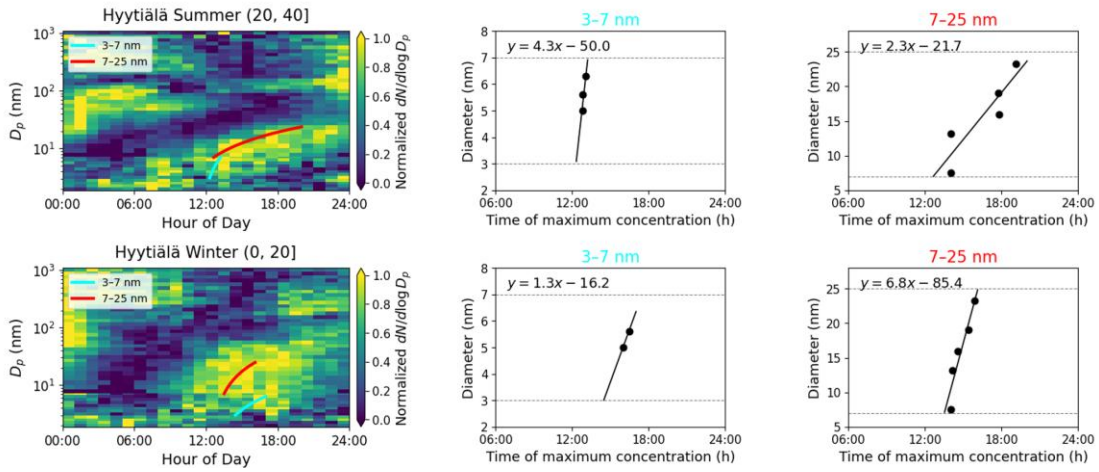

Figure S10. Example application of the maximum concentration method for deriving average particle growth rates (GRs) from normalized particle number size distributions at Hyytiälä. The upper row illustrates a relatively clear fitting case for the summer 20–40 % ranking interval, whereas the lower row illustrates a more uncertain fitting case for the winter 0–20 % ranking interval. The left panels show the normalized particle number size distributions, with the selected growth trajectories for the 3–7 nm and 7–25 nm size ranges indicated by colored curves. The middle and right panels show the corresponding linear fits between particle diameter and the time of maximum concentration for the 3–7 nm and 7–25 nm size ranges, respectively. The slopes of the fitted lines were used as the average GRs for the corresponding size ranges.

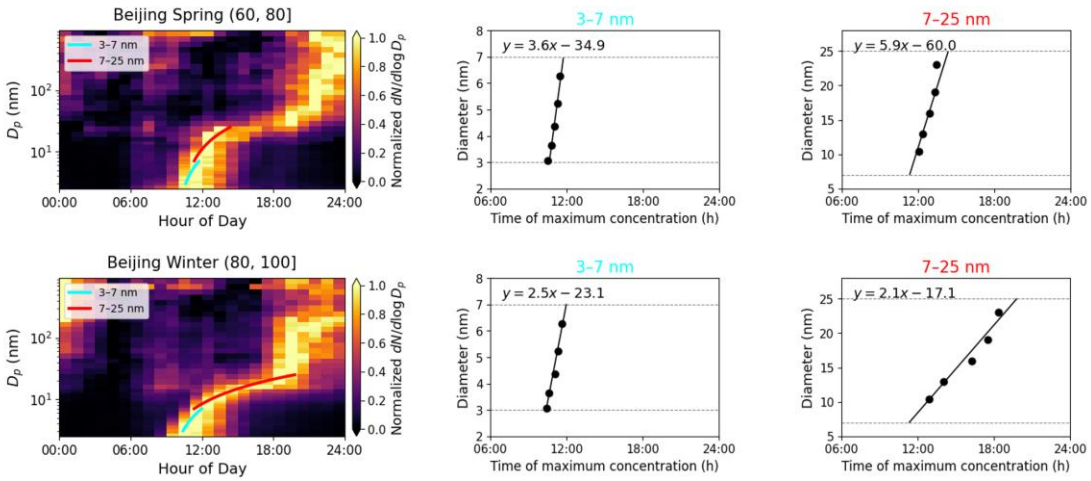

Figure S11. Example application of the maximum concentration method for deriving average particle growth rates (GRs) from normalized particle number size distributions at Beijing. The upper and lower rows illustrate clear fitting cases for the spring 60–80 % ranking interval and the winter 80–100 % ranking interval, respectively. The left panels show the normalized particle number size distributions, with the selected growth trajectories for the 3–7 nm and 7–25 nm size ranges indicated by colored curves. The middle and right panels show the corresponding linear fits between particle diameter and the time of maximum concentration for the 3–7 nm and 7–25 nm size ranges, respectively. The slopes of the fitted lines were used as the average GRs for the corresponding size ranges.